

**AFRL-SN-RS-TR-2005-408**  
**Final Technical Report**  
**December 2005**



# **WIDEBAND ELECTROABSORPTION MODULATOR FOR MICROWAVE PHOTONICS**

**University of California at San Diego**

*APPROVED FOR PUBLIC RELEASE; DISTRIBUTION UNLIMITED.*

**AIR FORCE RESEARCH LABORATORY  
SENSORS DIRECTORATE  
ROME RESEARCH SITE  
ROME, NEW YORK**

## **STINFO FINAL REPORT**

This report has been reviewed by the Air Force Research Laboratory, Information Directorate, Public Affairs Office (IFOIPA) and is releasable to the National Technical Information Service (NTIS). At NTIS it will be releasable to the general public, including foreign nations.

AFRL-SN-RS-TR-2005-408 has been reviewed and is approved for publication

APPROVED:       /s/

JAMES R. HUNTER  
Project Engineer

FOR THE DIRECTOR:       /s/

RICHARD G. SHAUGHNESSY, Chief  
Rome Operations Office  
Sensors Directorate

<b>REPORT DOCUMENTATION PAGE</b>			Form Approved OMB No. 074-0188	
Public reporting burden for this collection of information is estimated to average 1 hour per response, including the time for reviewing instructions, searching existing data sources, gathering and maintaining the data needed, and completing and reviewing this collection of information. Send comments regarding this burden estimate or any other aspect of this collection of information, including suggestions for reducing this burden to Washington Headquarters Services, Directorate for Information Operations and Reports, 1215 Jefferson Davis Highway, Suite 1204, Arlington, VA 22202-4302, and to the Office of Management and Budget, Paperwork Reduction Project (0704-0188), Washington, DC 20503				
<b>1. AGENCY USE ONLY (Leave blank)</b>		<b>2. REPORT DATE</b> DECEMBER 2005	<b>3. REPORT TYPE AND DATES COVERED</b> Final Sep 04 – Sep 05	
<b>4. TITLE AND SUBTITLE</b> WIDEBAND ELECTROABSORPTION MODULATOR FOR MICROWAVE PHOTONICS			<b>5. FUNDING NUMBERS</b> C - FA8750-04-1-0059 PE - 62204F PR - 516D TA - SN WU - 01	
<b>6. AUTHOR(S)</b> Paul K. L. Yu				
<b>7. PERFORMING ORGANIZATION NAME(S) AND ADDRESS(ES)</b> University of California at San Diego Office of Contract & Grant Administration 9500 Gilman Drive La Jolla California 92093-0934			<b>8. PERFORMING ORGANIZATION REPORT NUMBER</b>  N/A	
<b>9. SPONSORING / MONITORING AGENCY NAME(S) AND ADDRESS(ES)</b> Air Force Research Laboratory/SNDP 25 Electronic Parkway Rome New York 13441-4515			<b>10. SPONSORING / MONITORING AGENCY REPORT NUMBER</b>  AFRL-SN-RS-TR-2005-408	
<b>11. SUPPLEMENTARY NOTES</b>  AFRL Project Engineer: James R. Hunter/SNDP/(315) 330-7045/ James.Hunter@rl.af.mil				
<b>12a. DISTRIBUTION / AVAILABILITY STATEMENT</b> APPROVED FOR PUBLIC RELEASE; DISTRIBUTION UNLIMITED.				<b>12b. DISTRIBUTION CODE</b>
<b>13. ABSTRACT (Maximum 200 Words)</b> The objective of this grant was to determine experimentally the analog performance of the electroabsorption modulator (EAM) in external modulated RF fiber-optic links for radar and signal processing applications. UCSD investigated novel devices and material approaches, as well as novel electrode structures to enhance the RF link gain and spurious free dynamic range of link using the traveling wave electroabsorption modulator over a large bandwidth, operating at a nominal 1.55 um wavelength. In particular, high frequency, high saturation optical power analog Traveling Wave EAM (TW-EAM) waveguide modulators using peripheral coupled waveguide (PCW) were investigated and are reported here. An evaluation of the drive voltage of the TW-EAM, as well as the link gain and link SFDR was also accomplished. Finally an investigation of the segmented-electrode traveling wave EAM (STEAM) using a design that separates the optimization of the optical waveguide and the microwave transmission line is documented.				
<b>14. SUBJECT TERMS</b> Optical Modulator, Analog Optical Links, Electroabsorption Modulator, RF Optical Modulator			<b>15. NUMBER OF PAGES</b> 15	
			<b>16. PRICE CODE</b>	
<b>17. SECURITY CLASSIFICATION OF REPORT</b>  UNCLASSIFIED	<b>18. SECURITY CLASSIFICATION OF THIS PAGE</b>  UNCLASSIFIED	<b>19. SECURITY CLASSIFICATION OF ABSTRACT</b>  UNCLASSIFIED	<b>20. LIMITATION OF ABSTRACT</b>  UL	

## TABLE OF CONTENTS

Technical Objectives: .....	1
Overview: .....	1
1. Summary of accomplishments.....	2
1.1. High power PCW-IQW electroabsorption modulator .....	2
1.2. High power PCW-IQW photodetector .....	2
1.3. Fabrication of segmented traveling wave EA modulator (STEAM) .....	2
2. Technical progress achieved on project.....	3
2.1. High saturation power IQW-PCW electroabsorption (EA) modulator.....	3
2.2. Photodetector mode of the IQW-PCW EA modulator .....	6
2.3. Progress of the Segmented Traveling wave EA modulator .....	7
3. Conclusion and future plan.....	9
4. References. ....	9
5. Glossary for Acronyms.....	10
6. Publications .....	10

## LIST OF TABLES

FIGURE 1. TRANSFER CURVES AND MODULATOR PHOTOCURRENT CHARACTERISTICS OF SAMPLE 1 IQW PCW EA MODULATOR AT VARIOUS WAVELENGTHS. THE DEVICE HAS NO AR COATING. ....	3
FIGURE 2(A). SIMULATED ABSORPTION, REFLECTION AND TRANSMISSION SPECTRA OF THE EA WAVEGUIDE AT VARIOUS WAVELENGTHS, (B) MEASURED PHOTOCURRENT SPECTRA OF AN UNCOATED IQW-PCW WAVEGUIDE AT VARIOUS WAVELENGTHS AT ZERO BIAS. ....	4
FIGURE 3. MEASURED PHOTOCURRENT OF IQW-PCW EAM LINK, WITH THE MODULATOR AR COATED. THE INPUT OPTICAL POWER IS AT 18 dBm. ....	5
FIGURE 4. RF LINK GAIN VERSUS OPTICAL POWER FOR AN UNCOATED IQW-PCW EAM (SAMPLE 2) AT VARIOUS MODULATION FREQUENCIES. ....	5
FIGURE 5. THE PHOTOCURRENT GENERATED AT THE IQW PCW EA MODULATOR (SAMPLE 2) AS A FUNCTION OF BIAS VOLTAGE. ....	6
FIGURE 6. RESPONSIVITY OF THE IQW-PCW PHOTODIODE VERSUS INPUT POWER.....	7
FIGURE 7. SCHEMATIC LAYOUT OF THE SEGMENTED TRAVELING WAVE EA MODULATOR.....	8
FIGURE 8. PHOTOGRAPH OF THE SEGMENTED TRAVELING WAVE EA MODULATOR.....	9

## **Technical Objectives:**

The main technical objective/approach was to investigate high frequency, high saturation optical power analog TW-EAM waveguide modulator operating at 1.55  $\mu\text{m}$  wavelength using peripheral coupled waveguide (PCW) [1] combined with intrastep barrier quantum well (IQW) structure [2]. A second goal was the evaluation of the drive voltage of the TW-EAM, as well as the link gain and link SFDR. A third goal was the investigation of the segmented traveling wave EA modulator (STEAM) [3] using the design that separates the optimization of the optical waveguide and the microwave transmission line.

This report<sup>1</sup> details the University of California at San Diego (UCSD) efforts in a multi-year collaborative research program with AFRL at Rome Research Site who evaluated the EA modulators in fiber links.

## **Overview:**

The current year's program produced the following accomplishments:

1. Demonstration of a low link loss, lumped element electroabsorption modulator that combines peripheral coupled waveguide (PCW) and intra-step barrier quantum well (IQW). Transparent link gain is achieved at low frequencies.
2. Completed the first fabrication run of the STEAM which is advanced microwave electrode structure for the TW-EAM for impedance matching with the transmission line and loss microwave propagation loss. We have obtained preliminary results from the first fabrication run.
3. Collaborated with personnel at Rome Lab at the UCSD site in the fabrication and evaluation of EA modulators.

---

<sup>1</sup> The tasks reported in this project are also partially funded by DARPA.

## **1. Summary of accomplishments.**

### **1.1. High power PCW-IQW electroabsorption modulator**

1. For the first time, quantum well EA modulators reached optical powers as high as 200 mW.
2. The RF link gain of some of these EA modulators is larger than 0 dB at low frequencies.

### **1.2. High power PCW-IQW photodetector**

1. In the photodetector mode, the IQW-PCW modulator can deliver high photocurrent, the highest is at 100 mA.

### **1.3. Fabrication of segmented traveling wave EA modulator (STEAM)**

1. We have tested the fabrication procedure of the STEAM with ion implantation for electrical isolation between adjacent segments. Some preliminary measurements are done on these samples.

## 2. Technical progress achieved on project.

### 2.1. High saturation power IQW-PCW electroabsorption (EA) modulator

We have made two runs of IQW-PCW EA modulator in the duration of this program. Both are grown by MOCVD. The first sample consists of 8 quantum wells (5 nm intra step barrier + 6 nm well + 7 nm barrier layer) and a 1.63  $\mu\text{m}$  thick lower waveguiding layer. The quantum well is designed with exciton at 1.468  $\mu\text{m}$  wavelength. The second sample consists of 10 quantum wells (5 nm intra step barrier + 6 nm well + 7 nm barrier layer) and a 2  $\mu\text{m}$  thick lower waveguiding layer. The quantum well is designed with exciton at 1.484  $\mu\text{m}$  wavelength.

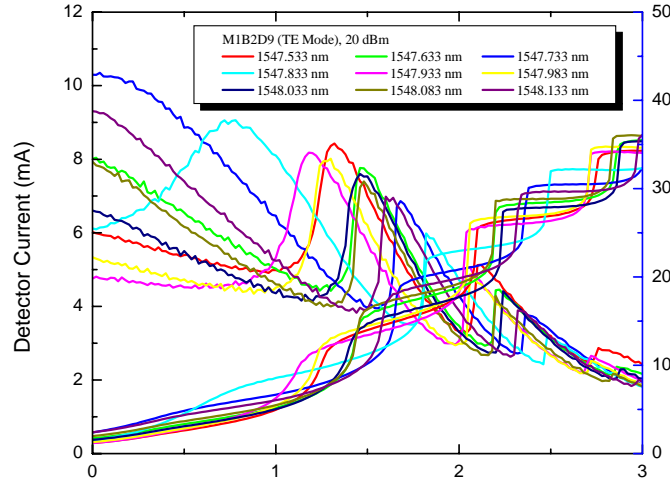
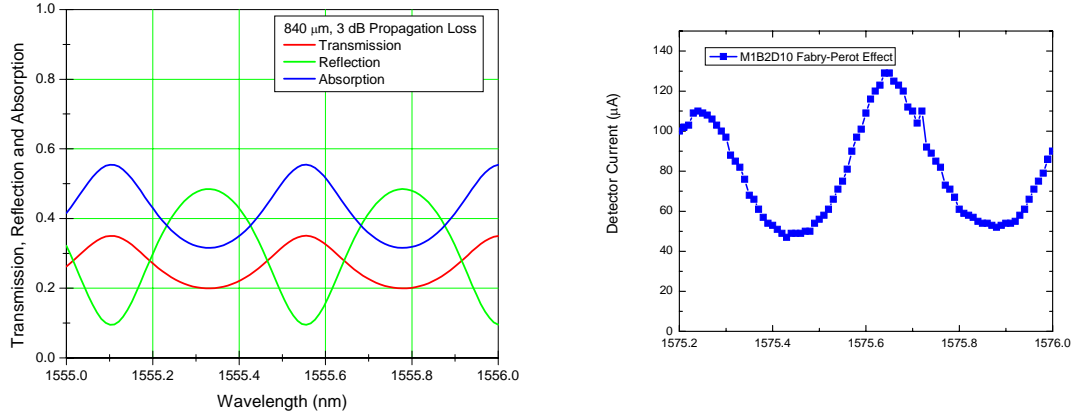


**Figure 1. Transfer curves and modulator photocurrent characteristics of Sample 1 IQW PCW EA modulator at various wavelengths. The device has no AR coating.**

The first sample was processed in lumped element modulator. These IQW PCW modulators have reverse breakdown voltage larger than 9 V and optical insertion loss  $\sim 7$  dB (facet to facet). The low propagation loss ( $< 1.2$  dB/mm) causes the Fabry-Perot effect to be significant (see Fig. 1) and masked the true transfer curve characteristics for devices without anti-reflection coating. The optical index of the layer structures, plus the small ridge width, resulted in a small confinement factor in the absorption layer. The transfer characteristic shows a higher  $V_{\pi}$  ( $> 2.8$  V). To confirm that the observed transfer



characteristics shown in Fig. 1 are due to Fabry Perot effect. We have measured the photocurrent spectrum, using a tunable wavelength laser, and compared with results with the calculation. The simulation results are shown in Fig. 2 a, which match closely with the measurement data, shown Fig. 2b.



(a)

(b)

**Figure 2(a). Simulated absorption, reflection and transmission spectra of the EA waveguide at various wavelengths, (b) measured photocurrent spectra of an uncoated IQW-PCW waveguide at various wavelengths at zero bias.**

The link gain of the uncoated device showed some abnormal behaviors and some device exhibits higher link gain at low frequencies. The frequency range over which high link gain is measured is very narrow, reminiscent of the Fabry Perot effect.

To minimize the Fabry Perot effect, we need to coat the facet with AR coating. Some devices from sample 1 were sent to a vendor for AR coating. The measured transfer curve of a device sample remains normal, at up to high optical power, as shown in Fig. 3. Because of the high  $V_{\pi}$  of this device, the maximum link gain is -12.5 dB at 18 dBm.

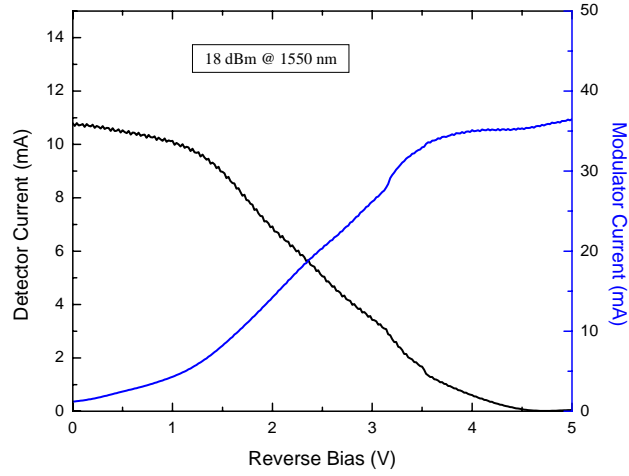


**Figure 3. Measured photocurrent of IQW-PCW EAM link, with the modulator AR coated. The input optical power is at 18 dBm.**

For the second IQW-PCW sample, the higher confinement factor at the active layer and the large number of wells resulted in a more effective modulation. Again, low propagation loss is observed in the waveguides and Fabry-Perot effect is observed for devices without coating. Fig. 4 shows the link gain versus optical power levels at different frequencies for the uncoated modulator.

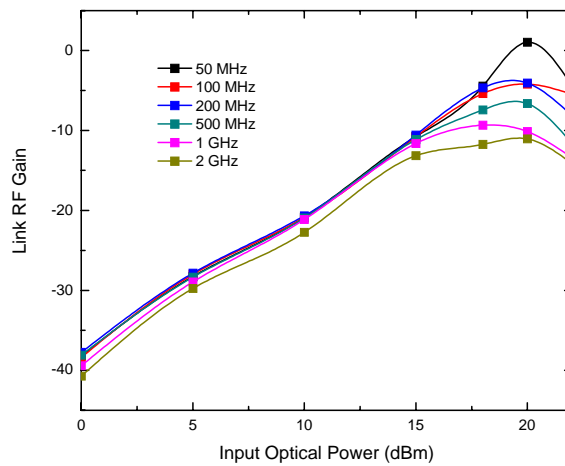


**Figure 4. RF Link gain versus optical power for an uncoated IQW-PCW EAM (sample 2) at various modulation frequencies.**

As in sample 1, we have sent out some of the devices of sample 2 for AR coating. For device that are  $> 0.6$  mm long,  $V_{\pi}$  of 1.2 to 1.4 V was achieved. Positive RF link gain was measured at low frequencies and the link gain has a RC frequency rolled-off as the lumped element electrode has limited bandwidth.

## 2.2. Photodetector mode of the IQW-PCW EA modulator

Due to electroabsorption effect that results in photogenerated carriers drifted in opposite directions, the EA modulator can function as an effective photodetector [4]. In this program, we also examine the high current capability of the IQW-PCW EA modulator.

In the photodiode mode, the device is biased at higher voltage than that for the modulator operation so as to obtain a high responsivity. Fig. 5 shows the photocurrent versus bias voltage for input optical power ranged from 1 mW to 100 mW, without the use of heat sink. The maximum quantum efficiency, at low optical power, is 0.8 A/W for the AR coated device.

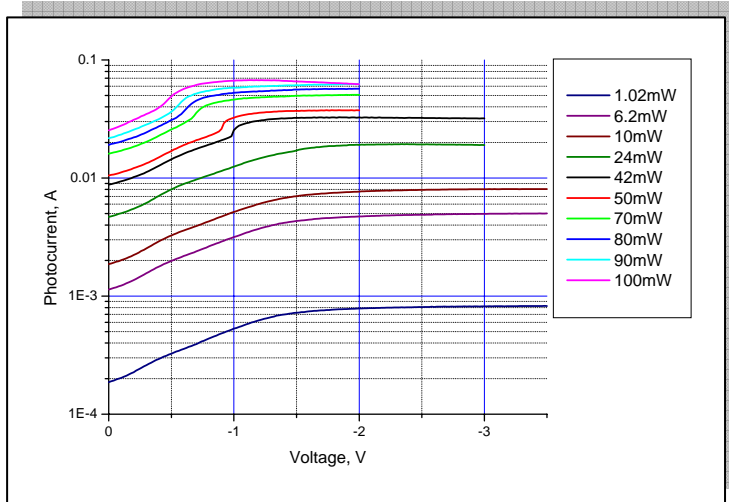


**Figure 5. The photocurrent generated at the IQW PCW EA modulator (sample 2) as a function of bias voltage.**

A plot of the responsivity is shown in Fig. 6, up to 100 mW input power. The responsivity is 0.5 A/W at 200 mW input, yielding a photocurrent of 100 mA. The drop in quantum efficiency at high power may be due to the heating effect in the device

induced by the photocurrent. Further investigation of the saturation behavior are on-going.

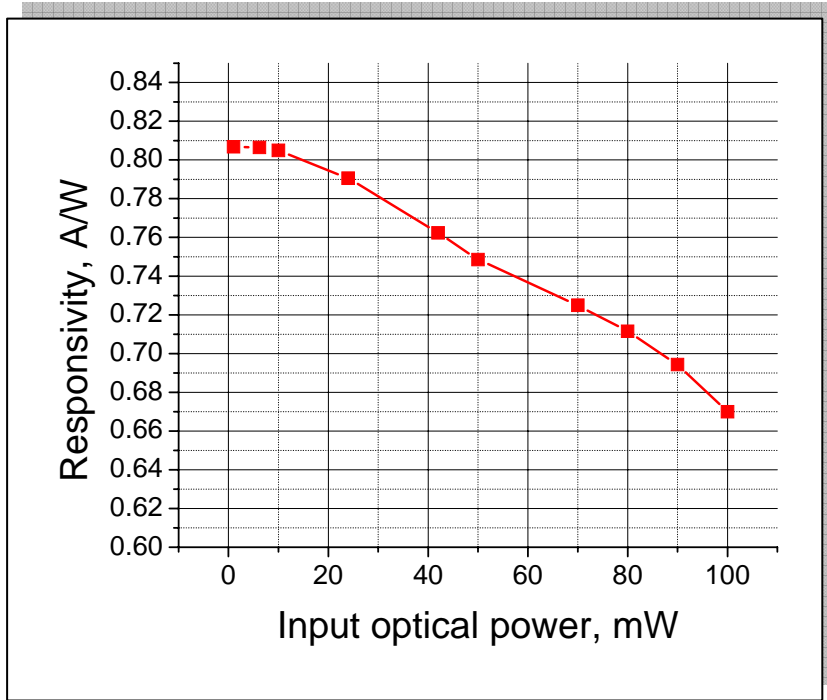


Figure 6. Responsivity of the IQW-PCW photodiode versus input power.

### 2.3. Progress of the Segmented Traveling wave EA modulator

The general requirements for traveling-wave electrodes are impedance matching, velocity matching, and low microwave loss. For traveling-wave EAMs, low-impedance matching is required, but velocity matching is not so important when the device is very short. However, with the consideration of PCW, a longer electrode ( $\sim 1$  mm) is required; there are certain advantages to use velocity matching traveling wave structures. It should be noted that the microwave velocities for transmission lines built on top of GaAs or InP are much faster than the optical group velocities in their optical waveguides, which is opposite to the case of traveling-wave  $\text{LiNbO}_3$  modulators.

The segmented traveling-wave design, described in last year's report, employs a separate transmission line that runs parallel to the optical waveguide, with its microwave velocity faster than the optical group velocity, and its microwave impedance higher than  $50 \Omega$  (the impedance of the microwave source). The modulation length (and its capacitance) in the

optical waveguide is segmented and periodically connected to the transmission line as capacitive loading, which lowers the microwave velocity and impedance. The goals are to match the lowered microwave velocity with the optical group velocity, and to match the lowered microwave impedance with  $50\ \Omega$  [3].

In this year's program, we have carried out the design in an EA modulator structure that uses MQW materials. Helium ion implantation is used to isolate the adjacent segment. The layout of the design is shown in Fig. 7. The on-chip resistor is for impedance termination and for connection to the ground (for the dc photocurrent).

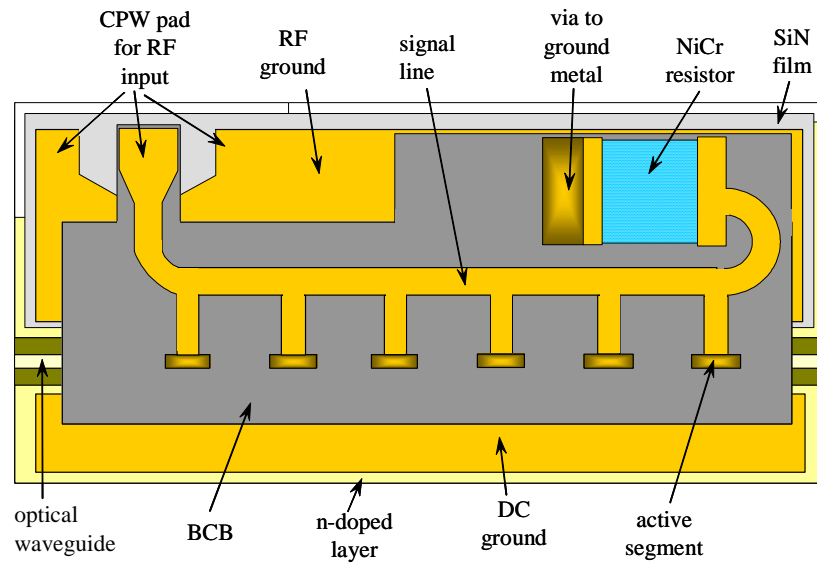


**Figure 7. Schematic layout of the Segmented Traveling Wave EA modulator.**

So far, we have made a fabrication run of the modulator (see Fig. 8 for the completed device) and has achieved the electrical isolation. The main difficulty is the number of mask steps involved and the inadequate information about the layers' optical and microwave indices. Preliminary measurements show low optical loss for the helium ion implanted region, as well as good transfer curve characteristics.

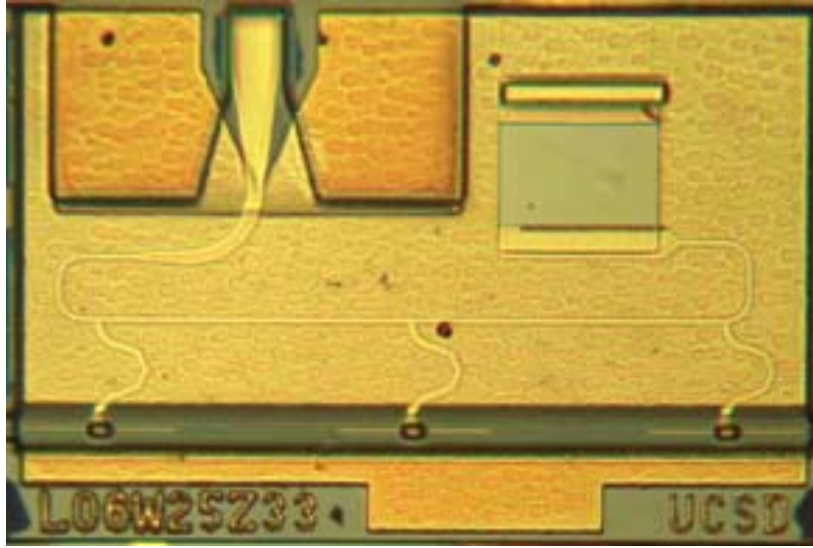


**Figure 8. Photograph of the Segmented Traveling wave EA modulator.**

### **3. Conclusion and future plan**

Under the support of the Air Force Research Laboratory, we have made important progress in this year in the fabrication and understanding of the IQW-PCW electroabsorption modulator for analog fiber links. While we have demonstrated low RF frequency modulators useful for transparent analog links, we look forward in the future program to realize experimentally the analog performance of both regular traveling wave electrode and segmented-electrode traveling wave electroabsorption modulator for higher frequency applications.

### **4. References.**

1. Y. Zhuang, W.S.Chang, and P.K.L. Yu, "Peripheral-Coupled-Waveguide MQW Electroabsorption Modulator for near transparency and high spurious free dynamic range RF fiber-optic Link, "IEEE Photonics Technology Letters, Vol. 16, No. 9, p. 2033-2035, 2004.
2. J.X. Chen, Y. Wu, W. X. Chen, I. Shubin, A. Clawson, W. S. C. Chang, and P. K. L. Yu, "High-Power Intrastep Quantum Well Electroabsorption Modulator Using

- Single-sided Large Optical Cavity Waveguide”, *IEEE Photonics Technology Letters*, Vol. 16, No. 2, p. 440-442, 2004.
3. G.L. Li, T.G.B. Mason, P.K.L. Yu, “Analysis of Segmented Traveling-Wave Optical Modulator,” *IEEE/OSA Journal of Lightwave Technology*, Vol 22, No. 7 p. 1789-1796, 2004.
  4. R. B. Welstand, S. A. Pappert, C. K. Sun, J. T. Zhu, Y. Z. Liu, and P. K. L. Yu, “Dual-Function Electroabsorption Waveguide Modulator/Detector for Optoelectronic Transceiver Applications,” *IEEE Photonics Technology Letters*, No. 8, 1540-1542, 1996.

## 5. Glossary for Acronyms

AR = anti-reflection

EA = Electroabsorption

IQW = Intra-step barrier Quantum Well

MOCVD = Metalorganic Chemical Vapor Deposition

MQW = Multiple Quantum Well

PCW = Peripheral Coupled Waveguide

SFDR = Spurious Free Dynamic Range

STEAM = Segmented Traveling wave Electroabsorption Modulator

TWEAM = Traveling Wave Electroabsorption Modulator

UCSD = University of California, San Diego

$V_{\pi}$  = half wave voltage; voltage to generate a  $\pi$  phase shift

## 6. Publications

1. “Transparent ROF link using EA modulators” by P. K. L. Yu, I. Shubin, X.B. Xie, Y. Zhuang, A. J. X. Chen, W. S. C. Chang, invited presentation at IEEE MWP 2005, in S. Korea.